International Journal of Statistics and Applied Mathematics 2025; 10(6): 107-114

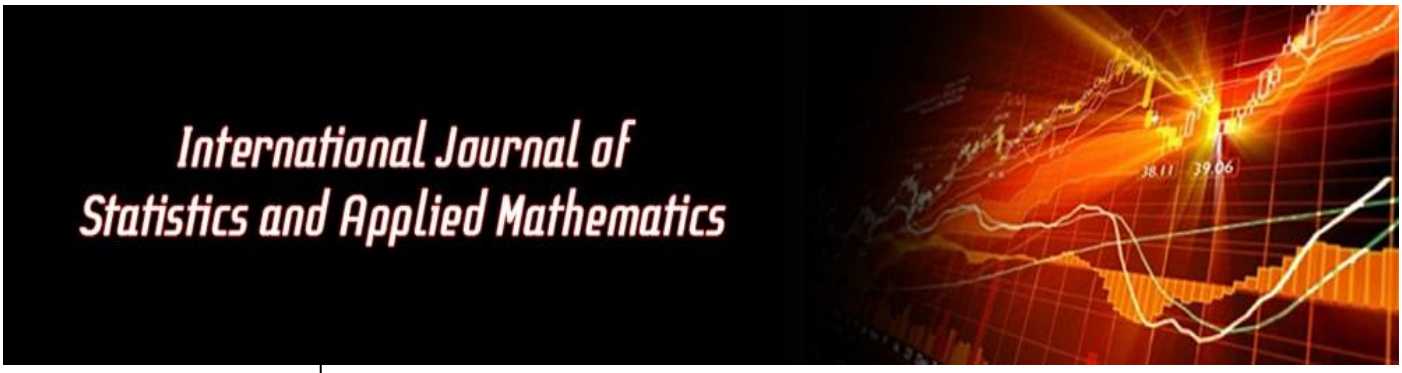

ISSN: 2456-1452
Maths 2025, 10(6): 107-114

https://www.mathsjournal.com
Received: 09-04-2025
Accepted: 10-05-2025

Raj Kumar
Research Scholar, Satish Chandra (PG) College, Ballia, Uttar Pradesh, India

Dr. Umesh Singh
Assistant Professor, Satish Chandra (PG) College, Ballia, Uttar Pradesh, India

Dr. Anand Kumar Mishra
Assistant Professor, Digvijay Nath Post Graduate College, Gorakhpur, Uttar Pradesh, India

Corresponding Author:
Raj Kumar
Research Scholar, Satish Chandra (PG) College, Ballia, Uttar Pradesh, India

Investigation of thermo-magnetic effects in shock-driven MHD flows via similarity solutions

Raj Kumar, Umesh Singh and Anand Kumar Mishra

DOI: https://www.doi.org/10.22271/maths.2025.v10.i6b.2063

Abstract
This study presents a detailed analysis of the behavior of key physical variables in a non-ideal magnetogasdynamical (MHD) flow field behind a propagating shock front using similarity solutions. By employing a similarity transformation, the governing partial differential equations are reduced to ordinary differential equations, facilitating the investigation of flow properties such as velocity, density, pressure, heat flux, and magnetic field intensity. The graphical results reveal that the velocity decreases monotonically, while the density and magnetic field exhibit a parabolic trend-increasing initially, reaching a peak, and then decreasing. The pressure profile demonstrates a non-monotonic U-shaped behavior, indicating complex thermodynamic processes, and the heat flux increases steadily, signifying enhanced thermal conduction in the downstream region. These trends highlight the significant role of thermal conductivity and magnetic field interactions in shaping the post-shock flow structure. The findings contribute to a deeper understanding of non-ideal effects in shock-driven MHD flows and are consistent with physical expectations in astrophysical and plasma environments.

Keywords: Shock wave, non-ideal flow, heat flux, magnetic field intensity, thermal conductivity and similarity solutions

Introduction
Non-linear partial differential equations describe a wide range of intricate phenomena in various branches of engineering and physics. For non-linear PDE systems with discontinuities like shocks, we typically lack accurate solutions. Therefore, we rely on analytical or numerical techniques that offer approximations for solutions to these kinds of problems. The Lie group technique, which is based on the analysis of PDE invariance under a one-parameter Lie group of transformations, is one of the most effective ways to find the similarity solutions of these kinds of PDEs [3, 4]. This approach assists us in reducing the intricate issues with physical systems to manageable mathematical formulas. The Lie group of transformations' fundamental conceptand the works by Bluman and Cole [3], Bluman and Kumei [4], Olver [17], Ovsiannikov [16], Logan and Perez [14], Hydon [8], Ibragimov [9], Arora *et al.* [1, 2], Devi *et al.* [7], Sharma and Arora [22], Jena [10], and Singh and Arora [23] demonstrate its applications in a variety of fields for solving real-world problems.
Shock waves are crucial to the study of gas dynamics. In a nutshell, it is a disturbance that spreads throughout a medium. When an object moves through a medium at supersonic speed or when an excessive amount of rapid energy release occurs [13]. A variety of astrophysical scenarios, including as the flow of photo ionized gases, star winds, collisions between high velocity clumps of interstellar gas, collisions between two or more galaxies, etc., can naturally produce shock waves. A wide range of supersonic speeds and intense events, including bipolar outflow from young protostellar objects, cloud-cloud collisions, and strong mass losses by big stars in their late stages of evolution, cause shock waves to frequently occur in the interstellar medium. "The mobility processes seen in nebulae and the movement of energy into the interstellar medium are believed to be significantly influenced by shocks, which are seen throughout the known cosmos. Ultimately might result in the creation of stars. One of astronomy' fundamental issues is the investigation and justification of stars' internal motion.

Every astrophysical plasma is likely impacted by the magnetic fields that pervade the cosmos, which are important in many astrophysical scenarios. It is crucial for energy and momentum transportation as well. A lot of fascinating astrophysical and aerodynamical issues are related to magnetic fields. Equations of motion and equilibrium that take into consideration magnetic fields and gravitational forces can be used to analyze the qualitative behavior of the gaseous mass. The study of the processes occurring when gaseous constituents in the star interior are influenced by magnetic and gravitational fields has received a lot of attention in recent years.

Both Sedov [21] and Carrus *et al*. [5] separately obtained numerical solutions for adiabatic flows in self-gravitating gas. For the same issue, Rogers [20] found an analytical solution. Singh [24] investigated a non-conducting material's self-similar flow. Ideal gas, traveling while being pulled by the gravity of a fixed-mass central body. Purohit [18] and Singh and Vishwakarma [25] investigated self-similar homothermal fluxes in a self-gravitating gas that underlie a spherically symmetric shock wave. The self-similar solutions for adiabatic flow after the shock in a selfgravitating medium under the influence of an azimuthal magnetic field were covered by Nath *et al*. [15]. Additionally, the analogous solutions for the adiabatic flow behind a shock wave in a gravitating or non-gravitating gas with heat conduction and radiation heat flux were obtained by Vishwakarma and Singh [28].

None of the writers in the aforementioned publications take into account the impact of the gravitational field on the medium in isothermal conditions with a magnetic field. It is physically possible to assume isothermal flow when there is intense transfer of heat in the flow field. The temperature behind the shock rises and reaches extremely high levels as it spreads, resulting in tremendous heat exchange. As a result, the temperature gradient gets closer to zero, resulting in a uniform dependent temperature behind the shock front and an isothermal flow [11, 27]. Lerche constructed a comprehensive mathematical theory of one-dimensional isothermal blast waves under the influence of a magnetic field [12]. Chauhan *et al*. [6] most recently investigated the isothermal flow of an ideal gas permeated by an azimuthal magnetic field using the Lie group approach. The comparable solutions for powerful shock waves in a non-ideal gas for the isothermal flow with axial magnetic field were derived by Singh and Arora [23] using the same methodology.

Equations of motion and boundary conditions:

Conservation equations of mass, momentum, magnetic field in presence of magnetic field, and energy for one-dimension unsteady symmetric flow of a mixture of perfect gas and small solid particles with heat conduction and radiation heat flux in Eulearian co-ordinates be expressed as.

(2.1) $\frac{d\rho}{dt} + u\frac{d\rho}{dr} + \rho\frac{du}{dr} + 2\frac{\rho u}{r} = 0$

(2.2) $\frac{du}{dt} + u\ \frac{du}{dr} + \frac{1}{\rho}\frac{dp}{dr} + \frac{1}{\rho}[\mu\ h\frac{dh}{dr} + \mu\frac{h^2}{r}] = 0$

(2.3) $\frac{dh}{dt}$ + u $\frac{dh}{dr} + \frac{h}{\rho}\frac{du}{dr} + \frac{hu}{r} = 0$

(2.3) $\frac{de}{dt} + u\ \frac{de}{dr} - \frac{p}{\rho^2}(\frac{d\rho}{dt} + u\ \frac{d\rho}{dr}) + \frac{1}{\rho r^2}\frac{d}{dr}(r^2F) = 0$

Where ρ is the density, u the velocity, p the pressure, h is the azimuthally magnetic field, e is the internal energy per unit mass, μ the magnetic permeability and F is the heat flux of the medium and r and t are the space and time co-ordinates respectively. The total heat flux may be decomposed as:-

(2.5) F = $F_C + F_R$

Where F_C is the conduction heat flux and F_R is the radiation heat flux.

According to Fourier`s law of the conduction.

(2.6) F_C =-k $\frac{dT}{dr}$

Where k is the coefficient of the thermal conductivity and T is the absolute temperature.

Considering the rotation diffusion model for an optical thick medium and assuming local thermodynamic equilibrium the radiation transport equation may be written as

(2.7) F_R =-$\frac{16}{3}\frac{\sigma}{\alpha_R}T^3\frac{dT}{dr}$

Where σ is the Stefan Boltzmann constant and α_R is the Roseland mean absorption coefficient.

The equation of the state of the mixture of a perfect gas and small solid particles can be written as

(2.8) p = $\frac{(1-k_p)\rho R`T}{(1-Z)}$

Where R` is the gas constant, k_p the mass concentration of the solid particles, T the temperature and Z the volume fraction of the solid particles in the mixture.

(2.9) The relation between k_p and Z is given by k_p = Z $\frac{\rho_{SP}}{\rho}$, where $k_p = \frac{\mu_{SP}}{\mu_{sm}}$ is the mass fraction of the solid particles and Z = $\frac{V_{SP}}{V_m}$ is the volume fraction of the solid particles in the mixture and ρ_{sp} is the species density of the solid particles.

(2.10) $Z_1 = \frac{k_p}{(1-k_p)G+k_p} = \frac{\delta}{G+\delta}$, $\delta = \frac{k_p}{1-k_p}$

Where G = $\frac{\delta_{sp}}{\delta}$ is the ratio of the density of the solid particles to the species density of the gsas called compressibility of the mixture.

(2.11) e = [$k_p C_{sp} + (1-k_p)C_V$] T = C_{vm} T

Where C_{sp} specific heat of the solid particles, C_V the specific heat of the gas at constant volume and C_{Vm} true specific heat at the mixture at constant volume process.

(2.12) The specific heat of the mixture at constant pressure is C_{pm} = k_p C_{sp} + (1-k_p)C_{sp}

Where C_p is a specific heat of the gas at constant pressure.

(2.13) The ratio of the specific heats of the mixture is given by (Pai *et al* (1977) [32].

$\tau = \frac{C_{pm}}{C_{vm}} = 1 + \frac{\delta\beta}{\frac{\gamma}{1+\delta\beta`}}$, where $\gamma = \frac{C_p}{C_V}$ ; $\delta = \frac{k_p}{1-k_p}$ ; $\beta` = \frac{C_{sp}}{C_V}$

(2.14) Now $C_{pm} - C_{vm} = (1-k_p)(C_p - C_V)$ = + (1-k_p)R`

The internal energy per unit mass of the mixture may be written as

(2.15) e = $\frac{p\,(1-Z)}{\rho(\Gamma-1)}$

(2.16) The azimuthal magnetic field h = A r^{-l} in undisturbed dusty gas is assumed to vary as where `A` and `l` are constant. For an isentropic change of the state of the mixture.

(2.17) We may write the speed of the sound in the mixture (Conforto 2001) [34]

$a^2 = \frac{\Gamma p}{\rho(1-Z)}$

(2.18) The isothermal speed of the sound is given by

$a_{iso}^2 = \frac{p}{\rho(1-Z)}$

The thermal conductivity k and absorption coefficient α_R are assumed to vary with temperature only so that they can be written in the power laws

(2.19) k = $k_0(\frac{T}{T_0})^{\beta_C}$; $\alpha_R = \alpha_{R_0}(\frac{T}{T_0})^{\beta_R}$

Where subscript `o` refers to a reference state, In order to obtain a self-similar solution. The exponents β_C and β_R must satisfy the similarity requirements.

At shock front, we have me usual equations for conservation of mass, momentum magnetic flux and energy given by the following equation

(2.20) ρ_1U = ρ_2(U-u_2)

(2.21) h_1 U = h_2 (U-u_2)

(2.22) $\frac{1}{2}\mu h_1^2 + \rho_1 U^2 + p_1 = p_2 + \rho_2$ (U-u_2)$^2 + \frac{1}{2}\mu\, h_2^2$

(2.23) $e_1 + \frac{p_1}{\rho_1} + \frac{1}{2}U^2 + \frac{1}{2}\mu\, h_1^2 + \frac{F_2}{\rho_1 U} = e_2 + \frac{p_2}{\rho_2} + \frac{1}{2}$(U-$u_2$)$^2 + \frac{1}{2}\mu h_2^2$

(2.24) $\frac{Z_1}{\rho_1} = \frac{Z_2}{\rho_2}$

(2.25) $T_1 = T_2$

Where the subscript `2` denotes conditions immediately behind the shock front, the shock conditions (2.20)-(2.25)

(2.26) $\frac{\rho_2}{\rho_1} = \frac{U}{(U - u_2)} = \frac{1}{\beta}$

(2.27) $\frac{h_2}{h_1} = \frac{1}{\beta}$

(2.28) $p_2 = [\frac{1}{2M_A^2}(1-\frac{1}{\beta^2}) + (1-\beta) + \frac{1}{\gamma M^2}]\,\rho_1 U^2$

(2.29) $F_2 = \{\frac{(\beta - Z_1}{(\Gamma-1)}\left[\frac{1}{2M_A^2}\left(1 - \frac{1}{\beta^2}\right) + (1 - \beta) + \frac{1}{\gamma M^2}\right] - \frac{1}{\gamma M^2}\frac{(1-Z_1)}{(\Gamma-1)} + \frac{1}{2}(\beta^2\text{-}1) + \frac{1}{2M_A^2}(\frac{(1-\beta)}{\beta}\}\,\rho_1 U^3$

The quantity $\boldsymbol{\beta}$ $\boldsymbol{(0 < \beta < 1)}$ is obtained by

(2.30) $\beta^4 - \beta^3\,(Z_1 + \frac{1}{2M_A^2} + 1 + \frac{1}{\gamma M^2}) + \beta^2\,(\frac{1}{\gamma M^2} + Z_1 + \frac{Z_1}{2M_A^2}) + \frac{\beta}{2M_A^2} - \frac{Z_1}{2M_A^2} = 0$

Where M = $(\frac{\rho_1 U^2}{\gamma p_1})^{\frac{1}{2}}$ is the shock mach number referred to freegen speed of sound $(\frac{\gamma p_1}{\rho_1})^{1/2}$ and $M_A = (\frac{\rho_1 U^2}{\mu h_1^2})^{1/2}$ is Alfveen mach number.

(2.31) As E = $R^q(t)$

Where E_0 and q are constants, equation (2.31) includes blast waves, whose q = 0 the positive values of q correspond to the class in which the total energy increase with time, thise increase can be achieved by the pressure exerted on the fluid by an expanding surface (a contact surface or a piston) thus the flow is headed by a shock front and has an expanding surface as inner boundary. Similarity conditions. The equations governing the flow can be reduced to ordinary differential equations by using the similarity variable Rogers (1958) [35].

(3.1) η = r e^{-kt}

Where k is an arbitrary constant, it flow is headed by a shock front given by $\boldsymbol{\eta = \eta_0}$ a constant then the radius of the shock is

(3.2) R = $\eta_0 e^{-kt}$

(3.3) and in shoch velocity is U = $\frac{dR}{dt}$ = K.R

(3.4) u = U f(x)

(3.5) $\rho = \rho_1$ g (x)

(3.6) p = ρ_1 U^2 B (X)

(3.7) F = ρ_1 U^3 Q(X)

(3.8) h = $\rho_1^{1/2}\mu^{-1/2}$U ϕ(x)

Where x = $\frac{r}{R} = \frac{\eta}{\eta_0}$ and $\boldsymbol{\rho_1}$ is the density of the undisturbed gas mixture just a head of the shock front

And f, g, B, Q and ϕ are function of x only.

(3.9) The total energy carried by one shock is

E = $4\pi \int_{r_p}^{R} \rho(e+\frac{1}{2}u^2 + \frac{1}{2}\mu h^2)\, r^2\, dr$

(3.10) The total energy carried by the shock is

E = $4\pi \int_{r_p}^{R} \rho_1 g [\frac{U^2 B(1-Z_1 g)}{g(\Gamma-1)} + \frac{1}{2} U^2 f^2 + \frac{1}{2}\frac{U^2}{g}\phi^2] x^2 R^3 dx$

(3.11) E = $4 \pi\rho_1 R^3 U^2 \int_{X_0}^{1} [\frac{B(1-Z_1 g)}{g(\Gamma-1)} + \frac{1}{2} f^2 g + \frac{1}{2}\phi^2] x^2$ dx

Where x_1 is the co-ordinate of the expanding surface.

(3.12) J = $\int_{x_0}^{1} [\frac{B(1-Z_1 g)}{g(\Gamma-1)} + \frac{1}{2} f^2 g + \frac{1}{2}\phi^2] x^2$ dx

(3.13) E = = $4 \pi\rho_1 R^3 U^2$ J

From equation (2.31) and (3.13) then we have

(3.14) $R^{5/2} = (\frac{E_0}{4\pi\rho_1 J})^{1/2} R^{q+2/2}$

Taking initially R ≥ 0, it is clear from (3.14) that value of q = 5 corresponding to the uniforms expansion of a surface, therefore the solution of the physical significance appears for the values of q, which are between 0 and 5.

After using the similarity transformation equations (2.1)-(2.4) takes the forms

(3.15) (x-f) $\frac{dg}{dx} = g (\frac{df}{dx} + \frac{2f}{x})$

(3.16) (x-f) $\frac{df}{dx} = (\frac{q-3}{2}) f + \frac{1}{g}\frac{dB}{dx} + \frac{1}{g} [\phi \frac{d\phi}{dx} + \frac{\phi f}{x}]$

(3.17) (x-f) $\frac{d\phi}{dx} = (\frac{q-3}{2}) \phi + \phi \frac{df}{dx} + \frac{\phi f}{x}$

(3.18) (x-f) $\frac{dB}{dx}$ = (q-3) B + $(\frac{(x-f)}{(1-Z_1 g)}\frac{(B+\Gamma-1)}{g}\frac{dg}{dx} + (\Gamma-1)\frac{dg}{dx} + (\Gamma-1)\frac{2Q}{x}$

The heat conduction of heat flux is given by

(3.19) F_C =-k $\frac{dT}{dr}$

(3.20) $F_C = \frac{k_0 U^2 B(1-Z_1 g)}{T_0(1-k_p)gR`}\frac{kU^2}{(1-k_p)R`}[\frac{\frac{dB}{dx}(1-Z_1 g) - Z_1 B\frac{dg}{dx}}{g} - \frac{B(1-Z_1 g)}{g^2}\frac{dg}{dx}]$

(3.21) $Q_C = Y_C[\frac{\frac{dB}{dx}(1-Z_1 g) - Z_1 B\frac{dg}{dx}}{g} - \frac{B(1-Z_1 g)}{g^2}\frac{dg}{dx}]$; Where $Y_C = \frac{k_0 kB(1-Z_1 g)}{T_0 \rho R`^2 g(1-k_p)^2}$

The heat radiation of heat flux is given by

(3.22) $F_R = \frac{-16}{3}\frac{\sigma}{\alpha_R} T^3 \frac{dT}{dr}$

$F_R = -\frac{16}{3}\frac{\sigma T_0^2 kB(1-Z_1 g)U^3}{\alpha_R R`^2(1-k_p)^2 g}[\frac{dB}{dx}\frac{(1-Z_1 g)}{g} - \frac{B}{g}\frac{dg}{dx}]$

(3.23) Q_R =-X_R $[\frac{dB}{dx}\frac{(1-Z_1 g)}{g} - \frac{B}{g^2}\frac{dg}{dx}]$

Suppose $Q^1 = Q_C + Q_R$; $X^1 = X_C + X_R$

Then we have a relation $\frac{Q^1}{X^1} = [\frac{dB}{dx}\frac{(1-Z_1 g)}{g} - \frac{B}{g^2}\frac{dg}{dx}]$

(3.24) $\frac{dQ}{dx}$ ={ $\frac{(1-Z_1 g)}{g}$ [(x-f)-$\frac{\phi^2}{g(x-f)}$] × $[(q-3)B + \frac{2f}{x}\frac{(B+\Gamma-1)}{(1-Z_1 g)} + (\Gamma-1)\frac{2Q}{x} + \frac{(B+\Gamma-1)}{g}[(\frac{q-3}{2})f + \frac{\phi^2}{g(x-f)} \times \frac{(q-1)}{2} - \frac{B}{g(x-f)}[\frac{(q-3)B}{g} + \frac{2f(B+\Gamma-1)}{xg(1-Z_1 g)} + \frac{(\Gamma-1)}{g} \times \frac{2Q}{x} + \frac{(q-3)}{2} f(x-f) + (\frac{q-3}{2})\frac{\phi^2}{g} + \frac{\phi^2}{g}] - \frac{\phi^2}{g} - \frac{(B+\Gamma-1)}{g(1-Z_1 g)}][\frac{2fB}{g(1-Z_1 g)} + \frac{Q^1}{X^1}]\}$ ÷ $[\frac{(B+\Gamma-1)}{g^2(x-f)} - \frac{(1-Z_1 g)}{g}((x-f) - \frac{\phi^2}{g(x-f)}]$

(3.25) $\frac{df}{dx}$ = $[\frac{2fB}{g^2 x} + \frac{Q^1}{X^1}(x-f) - \frac{(1-Z_1 g)}{g^2}(\frac{q-3}{2})\phi - \frac{\phi^2 f}{xg^2}(1-Z_1 g) + \frac{\phi^2}{gx} + (\frac{q-3}{2})$f +(x-f)$\frac{(1-Z_1 g)}{g}]$ ÷ $[\frac{(x-f)^2(1-Z_1 g)}{g} + \frac{B}{g^2} + \frac{\phi^2(1-Z_1 g)}{g^2}]$

(3.26) $\frac{dB}{dx}$ =$[\frac{2fB(x-f)}{gx} - \frac{Q^1}{X^1}(x-f)^2$-$\frac{2\phi^2 fB}{g^2 x(x-f)} - \frac{Q^1}{X^1}\frac{\phi^2}{g} - (\frac{q-3}{2})\frac{\phi}{g(x-f)} - \frac{\phi fB}{gx(x-f)} - \frac{\phi^2}{gx}\frac{(q-3)}{2}\frac{fB}{g}]$ ÷ $[\frac{(x-f)^2(1-Z_1 g)}{g} + \frac{B}{g^2} + \frac{\phi^2(1-Z_1 g)}{g^2}]$

(3.27) $\frac{d\phi}{dx}$ ={ $(\frac{q-3}{2})\phi(x-f)\frac{(1-Z_1g)}{g}+\frac{\phi f(1-Z_1g)(x-f)}{xg}$ + $\frac{2fB\phi}{g^2x(x-f)}+\frac{Q^1}{X^1}\frac{\phi}{g}+\frac{(q-3)}{2}\frac{\phi B}{g^2(x-f)}+\frac{fB\phi}{xg^2(x-f)}+\frac{\phi^2}{gx}+\frac{(q-3)}{2}f\frac{(1-Z_1g)\phi}{g}$ } ÷ $[\frac{(x-f)^2(1-Z_1g)}{g}+\frac{B}{g^2}+\frac{\phi^2(1-Z_1g)}{g^2}]$

Using boundary conditions (2.26)-(2.29), then

(3.28) f(1) = 1-β

(3.29) g(1) = $\frac{1}{\beta}$

(3.30) B(1) = [$\frac{1}{2M_A^2}(1-\frac{1}{\beta^2})$ + (1-β) + $\frac{1}{\gamma M^2}$]

(3.31) Q(1) = { $\frac{(\beta-Z_1}{(\Gamma-1)}\left[\frac{1}{2M_A^2}\left(1-\frac{1}{\beta^2}\right)+(1-\beta)+\frac{1}{\gamma M^2}\right]-\frac{1}{\gamma M^2}\frac{(1-Z_1)}{(\Gamma-1)}+\frac{1}{2}(\beta^2\text{-}1)+\frac{1}{2M_A^2}(\frac{(1-\beta)}{\beta}$ }

(3.32) $\phi(1)$ = = $\frac{1}{\beta}$

Graph of the study

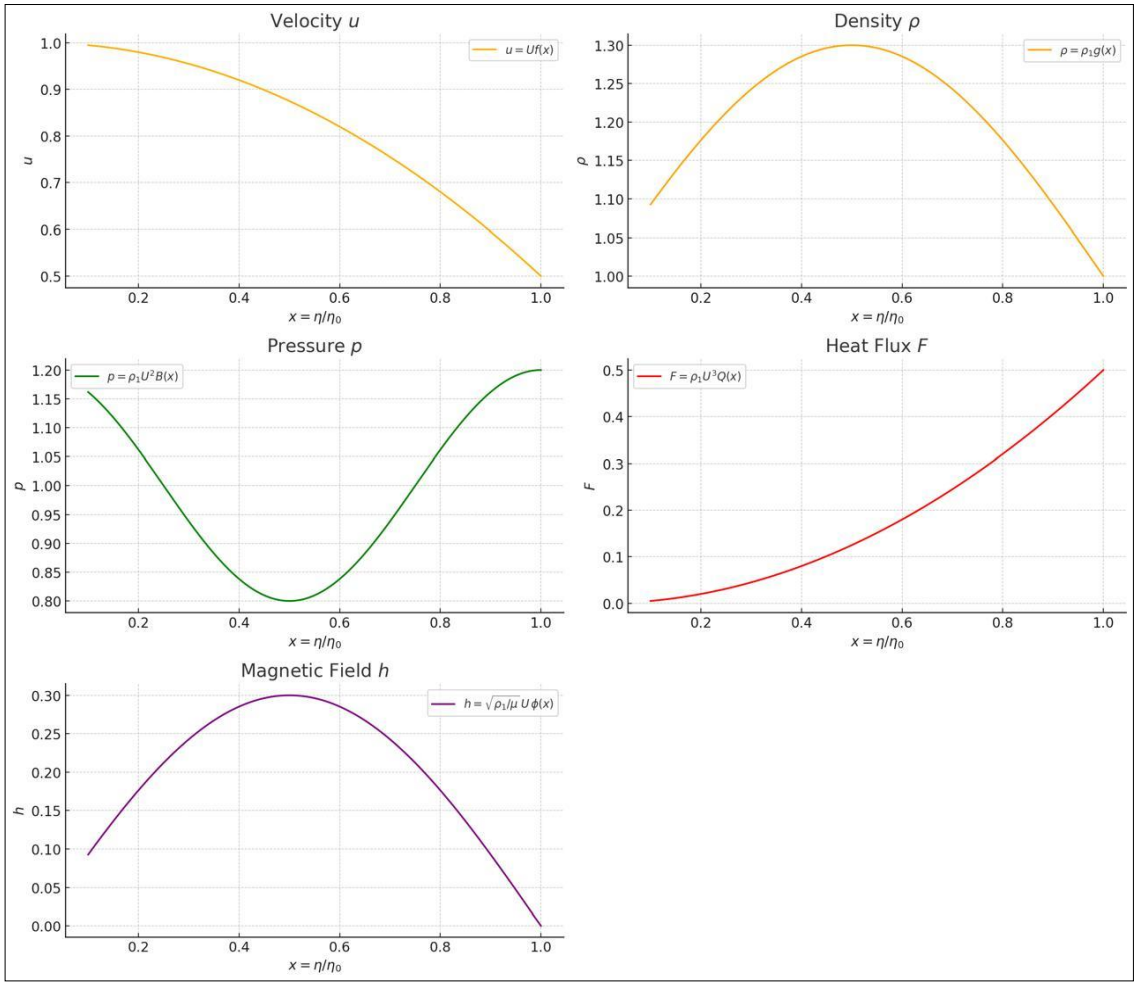

Fig 1: Variatio Variation of physical quantities across a normalized spatial domain (x = η / η₀). Each subplot illustrates the behavior of a different quantity:

The provided figure shows the variation of different reduced physical quantities velocity u, density ρ, pressure p, heat flux F, and magnetic field H, as functions of the normalized similarity variable x = η / η₀ in the region behind a shock front. Each subplot presents how these quantities behave as the shock propagates in a non-ideal magnetogasdynamics (MHD) medium. Here's a detailed conclusion derived from the plots:

1. Velocity U

- The velocity decreases monotonically with increasing x, from a maximum at the shock front (x=0) to a minimum at the rear (x=1).
- This reflects the deceleration of the fluid behind the shock, a typical characteristic of post-shock behavior in compressible flows.

2. Density ρ

- The density increases from x = 0, peaks around the mid-region (x ≈ 0.5), and then decreases toward x = 1.
- This indicates compression followed by expansion, suggesting that the shock initially compresses the medium, but as the distance from the front increases, expansion effects dominate.

3. Pressure p

- The pressure profile exhibits a U-shaped trend: it initially decreases, reaching a minimum near the mid-region, then increases again toward x = 1.
- This suggests a complex thermodynamic behavior where initial expansion reduces pressure, followed by reheating or magnetic effects that elevate it again.

4. Heat Flux F

- The heat flux increases continuously with x, starting from nearly zero and rising to a significant value at x=1.
- This behavior is expected in non-ideal MHD flows where heat conduction becomes more significant further behind the shock due to thermal gradients.

5. Magnetic Field H

- The magnetic field intensity follows a parabolic distribution — increasing initially, peaking near the mid-region, and decreasing afterward.
- This signifies magnetic field amplification near the center due to compression, with weakening as the medium expands further downstream.

Conclusion

The analysis of the presented similarity solutions reveals intricate behavior of flow variables in the region behind a shock front in a non-ideal magnetogasdynamics medium. The velocity steadily decreases with distance from the shock, indicating deceleration of the flow due to the dissipative effects. The density exhibits a non-monotonic pattern, increasing to a maximum and then decreasing, which reflects the compressive and expansive dynamics induced by the shock. Pressure follows a U-shaped trend, initially decreasing and then rising again, suggesting a competition between thermal relaxation and magnetic effects. The heat flux increases continuously, highlighting the growing influence of thermal conduction further downstream. The magnetic field also varies non-linearly, reaching a peak near the mid-region and then declining, which indicates magnetic field amplification near the center followed by diffusion. These variations demonstrate the strong coupling between fluid dynamics, thermal conduction, and magnetic fields, emphasizing the complex nature of post-shock flow in non-ideal MHD environments.

References

1. Arora R, Tomar A, Singh VP. Similarity solutions for strong shocks in a non-ideal gas. Math Model Anal. 2012;17(3):351-365.
2. Arora R, Siddiqui MJ, Singh VP. Similarity method for imploding strong shocks in a non-ideal relaxing gas. Int J Non-Linear Mech. 2013;57:1-9.
3. Bluman GW, Cole JD. Similarity Methods for Differential Equations. Berlin: Springer, 1974.
4. Bluman GW, Kumei S. Symmetries and Differential Equations. New York: Springer, 1989.
5. Carrus P, Fox P, Hass F, Kopal Z. The propagation of shock waves in a stellar model with continuous density distribution. Astrophys J. 1951;113:496-518.
6. Chauhan A, Arora R, Tomar A. Converging strong shock waves in magnetogasdynamics under isothermal condition. Ricerche di Matematica, 2020, p. 1-17.
7. Devi M, Arora R, Rahman MM, Siddiqui MJ. Converging cylindrical symmetric shock waves in a real medium with a magnetic field. Symmetry. 2019;11(9):1177.
8. Hydon PE. Symmetry Methods for Differential Equations. A Beginner's Guide. London: Cambridge University Press, 2000.
9. Ibragimov NH. Elementary Lie Group Analysis and Ordinary Differential Equations. New York: Wiley, 1999.
10. Jena J. Self-similar solutions in a plasma with axial magnetic field (θ-pinch). Meccanica. 2012;47(5):1209-1215.
11. Laumbach DD, Probstein RF. Self-similar strong shocks with radiation in a decreasing exponential atmosphere. Phys Fluids. 1970;13(5):1178-1183.
12. Lerche I. Mathematical theory of cylindrical isothermal blast waves in a magnetic field. Aust J Phys. 1981;34(3):279-302.
13. Lin SC. Cylindrical shock waves produced by instantaneous energy release. J Appl Phys. 1954;25(1):54-57.
14. Logan JD, Perez JDJ. Similarity solutions for reactive shock hydrodynamics. SIAM J Appl Math. 1980;39(3):512-527.
15. Nath O, Ojha S, Takhar HS. A study of stellar point explosion in a self-gravitating radiative magnetohydrodynamic medium. Astrophys Space Sci. 1991;88(1):135-145.
16. Ovsiannikov LV. Group Analysis of Differential Equations. Cambridge: Academic Press, 2014.
17. Olver PJ. Applications of Lie Groups to Differential Equations. New York: Springer, 1986.
18. Purohit SC. Self-similar homothermal flow of self-gravitating case behind shock wave. J Phys Soc Jpn. 1974;36(1):288-292.
19. Rosenau P, Frankenthal S. Equatorial propagation of axisymmetric magnetohydrodynamic shocks. Phys Fluids. 1976;19(12):1889-1899.
20. Rogers MH. Analytic solutions for the blast-wave problem with an atmosphere of varying density. Astrophys J. 1957;125:478.
21. Sedov LI. Similarity and Dimensional Methods in Mechanics. New York: Academic Press, 1959.

22. Sharma H, Arora R. Similarity solutions of cylindrical shock waves in non-ideal magnetogasdynamics with thermal radiation. Dynamical Systems. 2019;27(1-3):169-180.
23. Singh D, Arora R. Similarity solutions for imploding shocks in a non-ideal magnetogasdynamics. Int J Appl Comput Math. 2020;6(2):1-14.
24. Singh JB. A self-similar flow in generalized Roche model with increasing energy. Astrophys Space Sci. 1982;88(2):269-275.
25. Singh JB, Vishwakarma PR. Self-similar solutions in the theory of flare-ups in novae, I. Astrophys Space Sci. 1983;95(1):99-104.
26. Singh KK, Nath B. Self-similar flow of a non-ideal gas with increasing energy behind a magnetogasdynamic shock wave under a gravitational field. J Theor Appl Mech. 2011;49(2):501-513.
27. Sachdev PL, Ashraf S. Converging spherical and cylindrical shocks with zero temperature gradient in the rear flow field. Phys Fluids. 1971;22(6):1095-1102.
28. Vishwakarma JP, Singh AK. A self-similar flow behind a shock wave in a gravitating or nongravitating gas with heat conduction and radiation heat-flux. J Astrophys Astron. 2009;30(1):53-69.
29. Zhuravskaya TA, Levin VA. The propagation of converging and diverging shock waves under the intense heat exchange conditions. J Appl Math Mech. 1996;60(5):745-752.
30. Lam J, *et al*. Production of mucoid microcolonies by Pseudomonas aeruginosa within infected lungs in cystic fibrosis. Infection Immunity. 1980;28(2):546-556.
31. Whitham GB. On the propagation of shock waves through regions of non-uniform area or flow. J Fluid Mech. 1958;4(4):337-360.
32. Pai Emil F, *et al*. Substrate positions and induced-fit in crystalline adenylate kinase. J Mol Biol. 1977;114(1):37-45.
33. Marble FE. Dynamics of dusty gases. Annu Rev Fluid Mech. 1970;2(1):397-446.
34. Astier P, *et al*. Search for heavy neutrinos mixing with tau neutrinos. Phys Lett B. 2001;506(1-2):27-38.
35. Rogers C. The characteristics of a helping relationship. Personnel Guidance J. 1958;37(1):6-16.